Design of a modular and versatile interlock system for ultrahigh vacuum machines: A crossed molecular beam setup as a case study

Ying Guo, Xibin Gu, Ed Kawamura, and Ralf I. Kaiser
Department of Chemistry, University of Hawai'i at Manoa, Honolulu, Hawaii 96822

(Received 8 December 2005; accepted 15 January 2006; published online 14 March 2006)

The design of a modular, versatile interlock system for ultrahigh vacuum machines is presented. This system can monitor the pressure (ultrahigh vacuum and high vacuum), the status of the power (power failure, power fluctuations, and scheduled power outages), the operation mode of the pumps (operation versus failure), the flow of cooling water, the humidity and temperature levels in the laboratory, as well as the concentration of toxic gases. If any of the set points is triggered, the vacuum machine is protected fully automatically. The interlock system is also interfaced to an automated paging system, thus transmitting a pager signal to the person on duty. Since the interlock system is modular in nature, it can be expanded and be adapted stepwise to incorporate additional safety and monitoring functions as needed. © *2006 American Institute of Physics.*
[DOI: 10.1063/1.2173074]

I. INTRODUCTION

Crossed molecular beam experiments present the most versatile technique in the elucidation of the dynamics and of the energetics of elementary, bimolecular reactions.[1–12] In contrast to bulk experiments, where the reactants are mixed, the main advantage of the crossed beam approach is the capability to form the reactants in separate, supersonic beams. In principle, both reactant beams can be prepared in well-defined quantum states before they cross at a specific collision energy under the single collision conditions. The species of each beam are made to collide only with the molecules of the other beam and the products formed fly undisturbed towards the detector. These features provide an unprecedented approach to observe the consequences of a single collision event, preventing secondary collisions and wall effects. Crossed beam experiments can also help identify those intermediates involved and provide reaction products—critical input parameters in chemical reaction models of combustion[13] processes as well as of interstellar environments[14] and atmospheres of planets and their moons.[15]

Over the past decades, the use of crossed molecular beams has led to an unprecedented advancement in our understanding of fundamental principles underlying the chemical reactivity. Detailed experimental studies of simple chemical reactions consisting of three atoms have established experimental benchmark systems such as the reactions of chlorine,[16] deuterium,[17] and electronically excited nitrogen,[18] oxygen,[19] and sulfur[20] with molecular hydrogen. This approach has been extended also to tetra atomic systems such as OH/CO,[21] OH/H_2 together with their isotopic variants,[22] and CN/H_2 (D_2).[23] These simple systems are prototype reactions in bridging the theoretical understanding of reactive scattering via dynamics calculations on the chemically accurate potential energy surfaces (PESs) to experimental observations.[24] Although the theoretical and experimental interests in these light elementary reactions still continue[25] with the development of powerful theoretical models, attention is turning to the more complex systems of significant practical interest such as in combustion processes, chemical vapor deposition, catalysis, and chemistry in extreme environments (astrochemistry and planetary chemistry). These are, in particular, the reactions of atomic boron,[26] carbon,[27–31] nitrogen,[32] oxygen,[33] and transition metals[34,35] as well as of polyatomic radicals such as cyano (CN),[36,37] ethynyl (C_2H),[38] and phenyl (C_6H_5).[39]

The currently operating crossed beam setups differ primarily in the source geometry (fixed sources versus rotatable sources), in the intersection angle of the primary and secondary beams (variable angle versus fixed intersection angle), and in the detection scheme of the products [quadrupole mass spectrometric detector (QMS) with electron impact ionization or photoionization versus spectroscopic detection via a laser induced fluorescence (LIF)]. Molecular beam machines with nonrotating source chambers and beams intersecting perpendicularly are associated with the "universal" detectors. This detector type is rotatable within the scattering plane defined by both beams and consists of a triply differentially pumped ultrahigh vacuum chamber, a liquid nitrogen-cooled electron impact ionizer, and a quadrupole mass analyzer followed by a single particle monitor. Any reactively scattered species from the collision center after a single collision event takes place can be ionized in the electron impact ionizer, and, in principle, it is possible to determine the mass (and the gross formula) of all the products of a bimolecular reaction by varying the mass-to-charge ratio, m/z, in the mass filter. This detector makes it possible to map out the angular and velocity distributions of the scattered products. Measuring the time of flight of the products from the interaction region over a finite flight distance also obtains the product translational energy and angular distributions in the center-of-mass reference frame. Since the background rates at $m/z > 32$ are essentially zero, the sensitivity for the product detection is particularly high. Due to the universal electron impact ionization of the product, even species with unknown spectroscopic properties such as polyatomic, open shell hydrocarbon radicals can be detected. Different detector designs also exist, in which the quadrupole mass spectrometer is replaced by, for instance, a Rydberg tagging detector[22,40] or by a laser induced fluorescence (LIF) detection.[41] These detection schemes are restricted to hydrogen atoms and to small species such as the methylidene and hydroxyl radical, i.e., those with well-established fingerprints.

Some problems connected to the universal detector such as dissociative ionization of the product molecules, in particular, at commonly employed high electron energy in the electron impact ionizer of 200 eV, and background noise at certain m/z ratios from the residual gas in the ionizer region restrict the sensitivity of the method. This holds especially if low-mass hydrocarbon products have to be probed and the dissociative ionization of the parent molecules contributes significantly to the background at the low-mass hydrocarbon product of interest. This connects to the design of rotating source crossed molecular machines, in which both beams cross perpendicularly and where the triply differentially pumped quadrupole mass detector is fixed.[42,43] Although electron-impact ionization of the reactively scattered species is also feasible in these setups, the fixed detector geometry, using a tunable synchrotron radiation (8–18 eV), allows for the photoionization of the polyatomic products in the ionizer region.[42] Like electron impact ionization, the photoionization can be applied to any species, but provides a background-free universal product detection via soft vacuum ultraviolet (VUV) ionization, if the products with ionization potentials lower than that of the background species are monitored. Soft ionization by VUV light causes also less fragmentation of the parent ion, thus making the detection of the more complex reactions simpler. However, tunable synchrotron radiation of significant photon outputs, which is applicable in crossed beam studies, exists at only a few locations worldwide; this limits the available beam time to researchers. The development of pulsed lasers provided a viable alternative to photoionize, e.g., organometallic products in crossed beam reactions of transition metal atoms.[43] Very recently, a soft electron impact ionization—tuning the energy of the electrons over a range of 10–30 eV—provided a viable alternative to tunable VUV photo ionization.[44]

During the last years, much attention has been also devoted to the direct imaging of the scattered product distribution.[45] Both supersonic beams cross at a right angle, and the scattered products are photoionized (state selectively) on the axis of the Wiley-McLaren time-of-flight mass spectrometer. The ion cloud formed continues to expand with its nascent recoil velocity as it drifts through the flight tube. The ions then strike a position sensitive microchannel plate coupled to a phosphorus screen. The latter is viewed by a charge coupled device camera gated to record the signal at the mass of interest. The image is a two-dimensional projection of the three-dimensional product distribution which can be reconstructed to yield a product flux contour map. This provides a simultaneous detection of all recoil velocities, both speed and angle, for the product. In the early stages, ionimaging has suffered from limited velocity and angular resolution, largely determined by the dimensions of the interaction region compared to the detector and by blurring from the lensing effects associated with the grids. The recently developed velocity map imaging (VELMI) eliminates these limitations and replaces the conventional grids of the time-of-flight spectrometer with open electrostatic lenses.[46] This technique has been applied recently to investigate the reaction dynamics of electronically excited oxygen atoms $O(^1D)$ with molecular deuterium,[47] chlorine atoms with alcohols,[48] and of oxygen atoms with alkanes.[49,50]

However, due to the complexity of crossed molecular beam machines and interaction of multiple subunits of, for instance, vacuum system, detection systems, supersonic beams, and lasers, a catastrophic system failure is always imminent. Therefore, to protect the ultrahigh vacuum chambers, safety interlock systems are always advisable to protect the equipment and hence to minimize the experimental downtime. Various interlock systems for ultrahigh vacuum setups have been proposed,[51] but these units are neither universal nor modular in nature. In this article, we present the design of a truly universal and modular interlock system. We first present a brief description of the vacuum and operation principles of the crossed beam machine (Sec. II). This enables the reader to understand the design principles and modules of the interlock system (Sec. III). Although the design is discussed in the context of a crossed beam machine, due to its modular nature, it can be adapted to any vacuum system such as imaging machines, surface scattering vessels, and space simulation chambers.[52]

II. THE CROSSED BEAM MACHINE

The main chamber of the crossed beam machine consists of a 304 stainless steel box ($180\times160\times80$ cm^3; 2300 l; machining accuracy: ±0.03 mm) and is evacuated by three 2000 l s^{-1} magnetically suspended turbo molecular pump backed by a single scroll pump (10 l s^{-1}) to the low 10^{-8} torr region (Fig. 1). To minimize the background from straight-through molecules into the detector, the machine is also equipped with a cold shield located between the skimmers and interaction region. This oxygen-free high conductivity (OFHC) copper shield is interfaced to the second stage (10 K) of a cold head [4500 l s^{-1} (water); 1500 l s^{-1} (nitrogen/oxygen)] and improves the vacuum in the main chamber to 4×10^{-9} torr. This arrangement keeps the pressure in the main chamber during an actual experiment to 10^{-7} torr (continuous sources) and 5×10^{-8} torr (pulsed sources). Two source chambers are located inside the main chamber; in its current geometry, both beams cross perpendicularly; in the future, the secondary source will be rotated to vary the intersection angle of the crossing beams to yield collision energies of the reacting particles between 0.3 and 150 kJ mol^{-1}. Each source chamber is pumped by a 2000 and a 430 l s^{-1} maglev pump to the medium 10^{-9} torr region; operating pulsed and continuous sources increases the pressure to about 10^{-5} and 10^{-4} torr, respectively. All maglev pumps require no maintenance and are hydrocarbon free. A

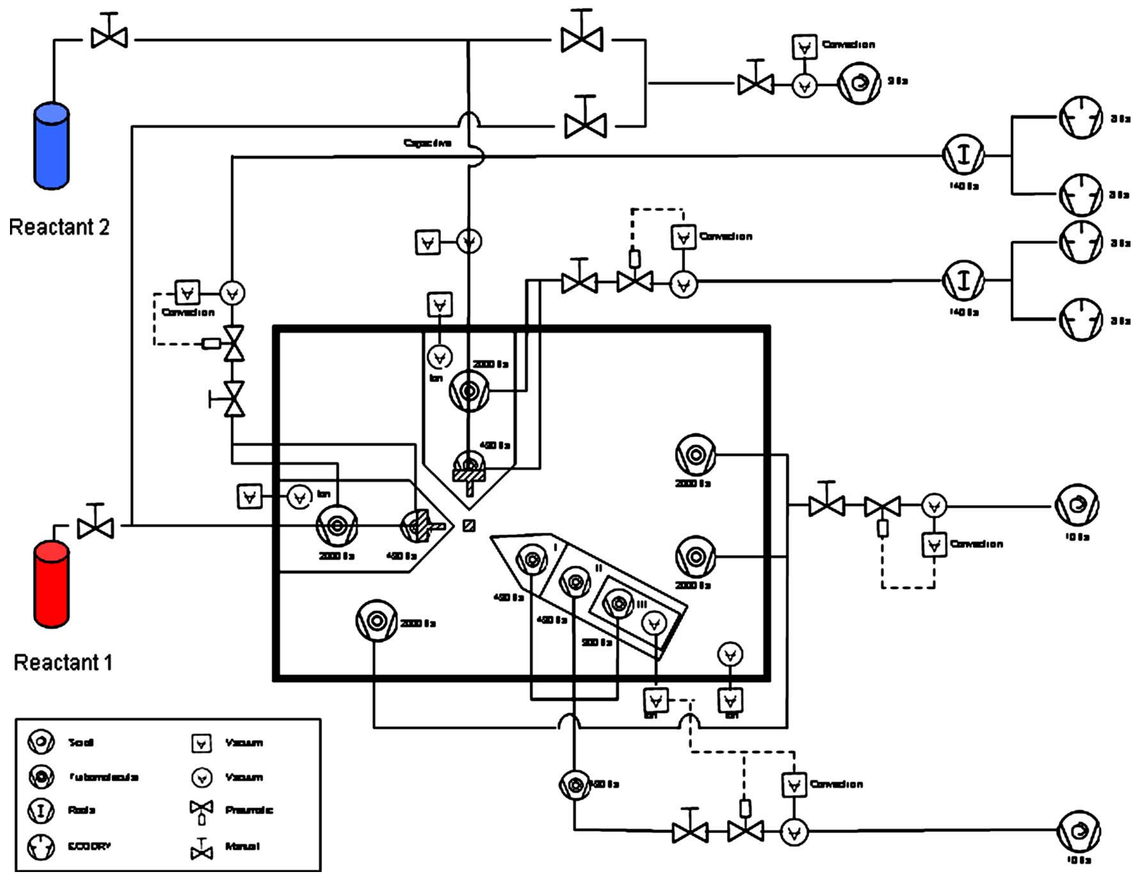

FIG. 1. Pumping scheme of the crossed beams machine. Chopper wheels are omitted for clarity.

dry roots pump ($140\ \mathrm{l\ s^{-1}}$) roughed by two oil-free EcoDry pumps ($16\ \mathrm{l\ s^{-1}}$) backs the turbo pumps of each source chamber. To minimize the outgasing of the sealing material, copper gaskets are used preferentially. Whenever the O rings are used (detector entrance port, laser entrance window, and main door), these are teflon coated and differentially pumped by an oil-free pumping station at 10^{-7} torr to ensure the 4×10^{-9} torr in the main chamber.

The reactively scattered species are monitored using a quadrupole mass spectrometer. Actually, the detector is located in a separate, triply differentially pumped ultrahigh vacuum chamber and is rotatable within the plane defined by both beams. Since every rotation in a vacuum system will increase the pressure inside the system, the rotating detector ring is separated by three teflon loaded seals from the atmosphere. The spaces between these seals are doubly differentially pumped to reduce the pressure from the atmosphere (760 torr) via 10^{-2} and 4×10^{-8} torr (teflon sealed regions) to 4×10^{-9} torr in the main chamber. This arrangement ensures no pressure increase in the main chamber even if the detector is being rotated. Note that the detector platform moves down by 0.28 mm when the main chamber is evacuated: therefore, the alignments of the detector apertures have to be carried out under vacuum but not at atmospheric pressure. Also, the liquid nitrogen shield (region III) moves up by 1.42 mm due to the contraction; hence, the alignment of aperture III has to be conducted under the liquid nitrogen-cooled conditions. Differentially pumped detector regions I/II reduce the gas load from the main chamber, whereas region III contains the Brink-type electron impact ionizer, surrounded by a liquid nitrogen cold shield (liquid nitrogen consumption: 80 l/day). The quadrupole mass filter and the Daly-type scintillation particle detector are connected to region II. Here, extracted ions are focused by an electric lens located after the extractor plate enter the ionizer exit aperture, pass the quadrupole mass filter, and are accelerated towards a stainless steel target coated with a 200 nm aluminum layer maintained at −25 kV. The ion hits the surface and initiates an electron cascade which is accelerated by the same potential until they reach an aluminum coated (200 nm) organic scintillator whose photon cascade is detected by a photomultiplier (PMT) mounted outside the UHV detector. Note that each region is pumped by a magnetically levitated turbo molecular pump (regions I/II: $430\ \mathrm{l\ s^{-1}}$; region III: $300\ \mathrm{l\ s^{-1}}$); all three pumps are backed by a $430\ \mathrm{l\ s^{-1}}$ turbo molecular pump whose exhaust is connected to an oil-free scroll pump ($10\ \mathrm{l\ s^{-1}}$). This pumping scheme reaches down to the low 10^{-11} torr in region III; lower pressures can be achieved by operating a cold head inside region III (4 K; 1.5 W). A slide valve with the Kalrez O ring is used to separate the main chamber from the first differentially pumped detector region. The regions are separated by rectangular apertures of $4.06\times4.06\ \mathrm{mm^2}$ (main chamber–region I), $5.21\times5.21\ \mathrm{mm^2}$ (region I–region II), and $5.84\times5.84\ \mathrm{mm^2}$ (region II–region III). We can compare our vacuum in region III with the theoretically available low pressure limit. The pressure in the nth differentially pumped region, p_n, calculates via Eq. (1). Here, p_o represents the pressure of the main

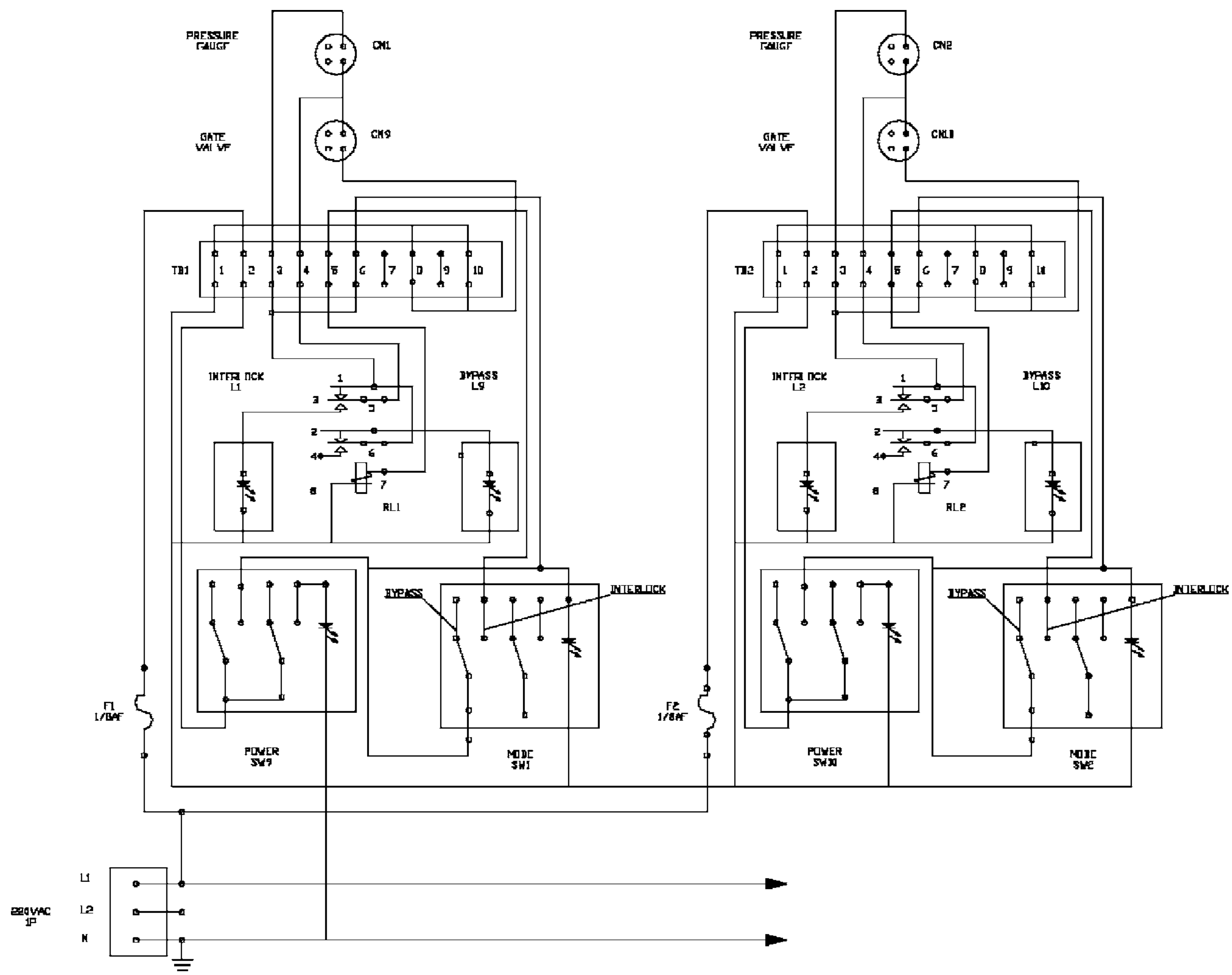

FIG. 2. Circuit diagram of one unit of the main chamber vacuum interlock module.

chamber, $\bar{v}_o$ is the averaged thermal velocity of the background molecules entering the detector from the main chamber, A_i is the aperture size, and $S_{i,\mathrm{eff}}$ is the effective pumping speed. Accounting for the experimental setup, a pressure as low as 5×10^{-14} torr should be available; this calculation assumes a main chamber pressure of 10^{-7} torr during the experiments and neglects outgasing of the stainless steel material (producing mainly carbon monoxide and molecular hydrogen) and the vapor pressure of the thoriated iridium filament. During on-axis operation (beam characteristics) a small detector aperture of 0.25 mm is used, whereas off-beam-axis scattering experiments require a larger, 3.81×3.81 mm^2 rectangular aperture. Here, the 5.8×5.8 mm^2 rectangular aperture of region III constrain the viewing angle of the ionizer defining the detector acceptance angle to $6.7\pm0.2\times10^{-4}$ sr.

$$p_n = \frac{p_o(\bar{v}_o^n)}{4^n}\prod_{i=1}^{n}\frac{A_i}{S_{i,\mathrm{eff}}}. \tag{1}$$

III. THE INTERLOCK SYSTEM

The design of the crossed beam machine dictates the requirements of the interlock modules. Here, we elucidate on the requirements to interlock and to monitor the following conditions of the crossed beam machine: (1) pressure (vacuum), (2) power (power failure, power fluctuations, and scheduled power outages), (3) pump status (operation versus failure), (4) cooling water, (5) humidity level, (6) temperature level, and (7) the accidental release of toxic reactant gases.

A. Pressure interlock module

The breach of the vacuum system probably presents the most common hazard to vacuum vessels. The loss of the (ultra) high vacuum originates either from a malfunctioning pump (main pump or backing pump), a power failure (all pumps stop operating), and/or from a leaking window—often a magnesium fluoride or fused silica—of a laser beam entrance port. A rapid gas entry can result in a catastrophic turbo molecular pump failure since the gas may induce the rotor blades to collide with the stator. Also, a cold head (main chamber; region III) and liquid nitrogen shield (region III) operating under these conditions inside the vacuum system, presents a particular risk; the leaking gas—water vapor in particular—can condense on the 10 and 50 K stages; if the vacuum breach occurs overnight and the cold head is still in operation, the experimentalist might discover an *ice box* in-

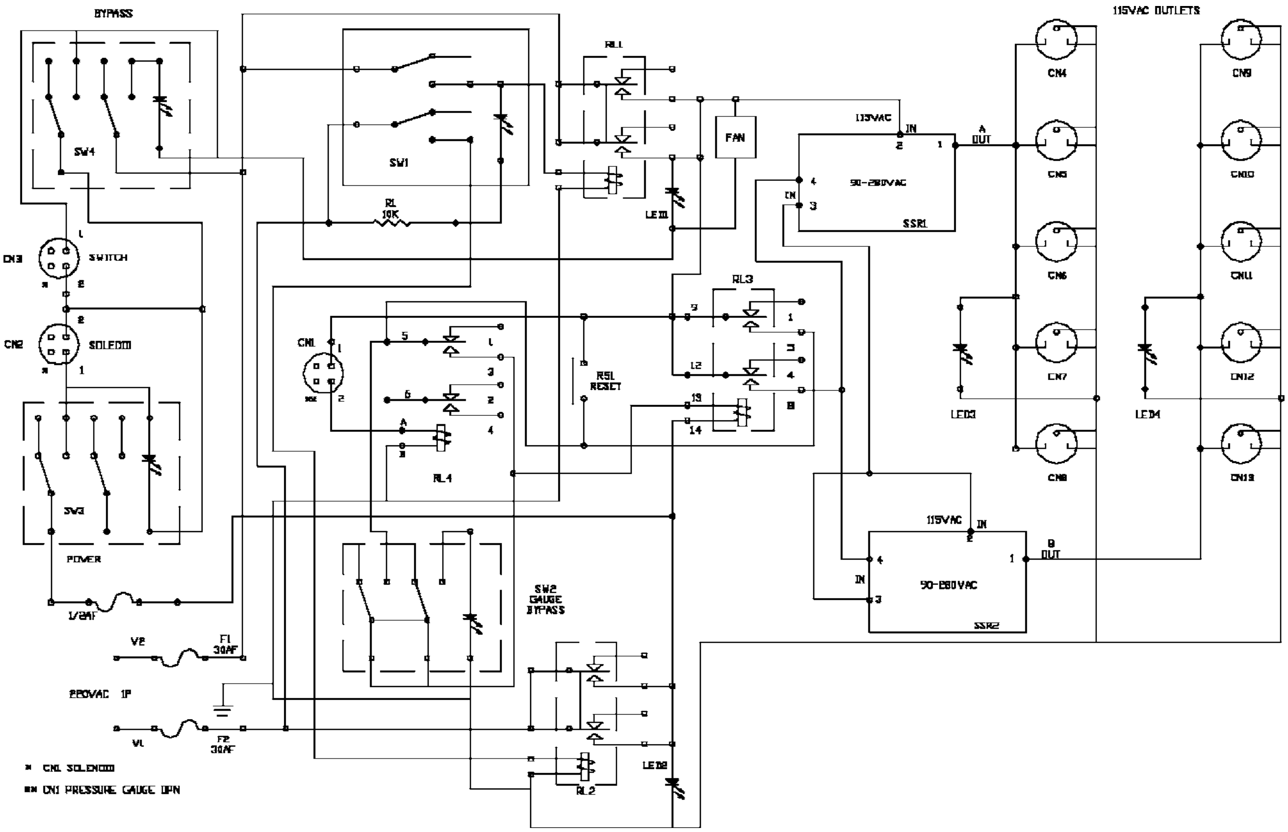

FIG. 3. Circuit diagram of the detector vacuum interlock module.

side the vacuum system the next day. Also, vacuum leaks can result in strong gas discharges and ultimately in a destruction of the power supplies and detector system, since the voltages to the photomultiplier (–1500 V), quadrupole rods (4000 V), and Daly detector (–25 kV) are fed via electrical feedthrough from the atmospheric side to the main chamber and to region II of the detector. Finally, a vacuum leak can simply result in a burnout of the thoriated iridium filament of the Brink ionizer nested inside region III. Therefore, it is advisable to separate first the main turbo molecular pump from its backing pump unit by a fast shutting, pneumatic gate valve (Fig. 1). Considering the main chamber and both source regions, a convectron gauge is placed between each backing pump unit and the pneumatic gate valve. The design of the Terranova 926 Dual Convectron Controller incorporates programmable set points; if the pressure rises beyond the set point—typically a few tens of mtorr—a relay contact opens and cuts the power to the pneumatic valve. In a similar manner, a convectron gauge and a fast shutting gate valve can be located between the laser entrance window. The gate valves together with the convectron controllers easily eliminate vacuum breaches from power, pump, and window failure. However, the interlock of the detector system is more complicated and cannot utilize a convectron gauge to trigger the shut down of the pneumatic valve. Here, a Stable Ion Gauge and 370 Granville Phillips Controller monitor the pressure in the UHV region (III) of the detector. This unit has an integrated process control board to select the set point of the relay contact to 1×10^{-10} torr. If the pressure increases beyond the set point, a fast shutting gate valve isolates the detector from the backing pump. However, since the pressure increase can also result in the partial destruction of the detector and the power supplies (filament burnout; high voltage arcing), the power to the ionizer, Daly detector, and PMT tube is cut as well. The circuit diagrams for the pressure and detector interlock modules are presented in Figs. 2 and 3, respectively.

B. Power interlock module

To maintain the ultrahigh vacuum in case of power failure, power fluctuations, and scheduled power outages, it is desirable to hook up the pumps (turbo pumps and scroll pumps), interlock systems, pressure gauges, gate valves, liquid nitrogen station, and the detector power supplies to an array of uninterruptible power supply (UPS) units. Here, the crossed beam setup is powered by five Liebert CXT UPS systems. Each UPS system is rated for 5 kVA and supplies—supported by additional battery units—the power to the machine for about 90 min. Each unit also has an integrated automatic voltage regulator (AVR) to filter power spikes which otherwise could damage the magnetically levitated pumps. However, due to the limited backup time, the UPS systems are of limited use in case of extended power failures (scheduled power outages, catastrophic power grid failure). To account for this scenario, all critical components associated with the UHV detector system of the machine are hooked up to a single UPS system. To maintain the UHV conditions, a manual switch can transfer the power from the main power grid to the fuel powered Honda generator. This

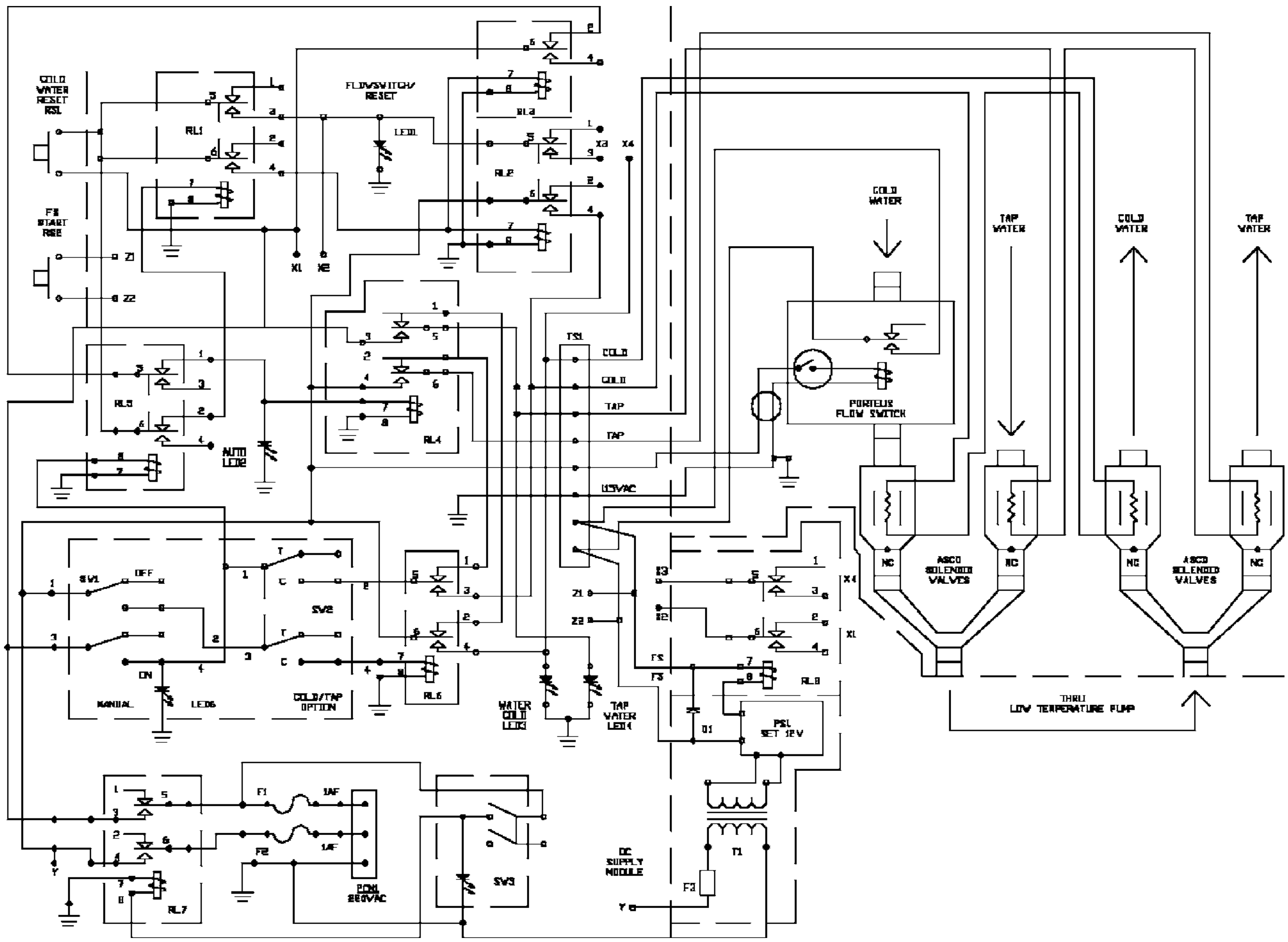

FIG. 4. Circuit diagram of the water flow interlock module.

unit generates up to 6 kVA power which can be fed—via an automatic voltage regulator—into the dedicated UPS system supporting the critical detector power. Since the actual power consumption of the detector system is only about 3 kVA, the generator also recharges the UPS system automatically; this presents an additional safety feature if the generator malfunctions.

C. Water flow interlock module

To minimize any negative effects from a malfunctioning closed cycle water chiller, all pumps in our crossed beam machine are air cooled via convection. Only two units (the cold heads in the main chamber and in the detector) require water cooling. The cold head operating in region III presents a particular hazard potential. If the water flow stops, the thermal sensor inside the cold heat power supply unit triggers a shutdown of the cold head. Since the latter is loaded with gas condensates, a thawing cold head would increase the pressure in region III dramatically beyond the 1×10^{-10} torr set point to shut the pneumatic valve and the power to the ionizer. To avoid this problem, we designed an automatic transfer unit which can switch the cooling water loop from the chiller unit to tapped water (Fig. 4). Here, four solenoid valves[53] are teed pairwise to the cooling water inlet and the outlet of the cold head compressor unit. The inlet is connected to the water chiller (cold water) and to the tapped water (tap water). The outlets are connected to the chiller (cold water) and to the drain (tap water). A flow switch[54] located between the chiller and the cold water inlet valve monitors the flow rate of the water. If the flow drops below a specified set point (in this case, the compressor would shut down due to overheating), the water flow interlock module automatically opens both valves connected to the tapped water and closes—time delayed—the solenoid valves to the chilled water system (Fig. 4). This ensures a cooling of cold head even if the chiller system sustains heavy damage and stops operating.

D. Central monitoring system

Even if the interlock modules (pressure, power, and water flow) can protect a UHV system from harsh damage, these units are only of limited value, if the information of a system failure cannot be transmitted to the user. Assuming the interlock modules are connected to an acoustical alarm (bell), the laboratory personnel can undertake appropriate steps if a malfunction occurs during normal laboratory operation hours. However, if a break down takes place during off-duty hours, the operation personnel has to be notified automatically. This is carried out here by interfacing the pressure, power, and water interlock modules to an automated pager system. In detail, the serial output signal of each of the UPS systems is fed into the central monitoring system

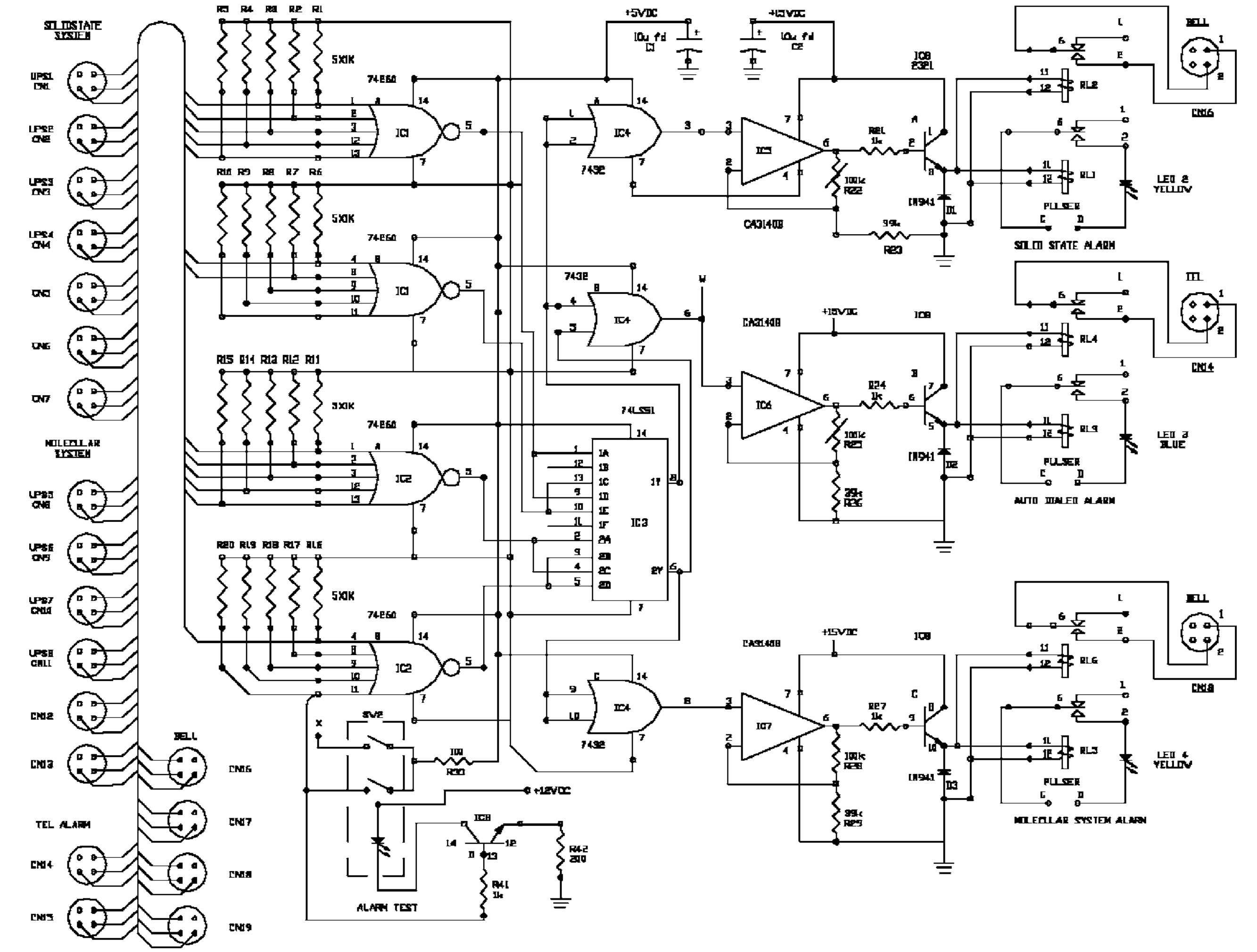

FIG. 5. Circuit diagram of the central monitoring module.

(Fig. 5); in case of either a power or UPS failure, a normally open relay located inside the Liebert UPS closes automatically. We designed a logic circuit[55] so that if any of the five relays closes, the power to a dedicated 110 V socket shuts down. A Liebert Power Sure UPS (500 V A), which powers a personal computer, is connected to this socket. The computer is connected via a serial interface to the Power Sure UPS system and monitors the status of the latter via a freely available MULTILINK software package continuously. If the software detects power fluctuations or a shutdown to the Liebert Power Sure, an automated page is activated to the person on duty.[56] In summary, cutting the power to the 110 V outlet translates into an activation of the MULTILINK software triggered pager system. So far, we have only focused on the power interlock module. However, we can expand the logic circuit in a modular way so that the 110 V outlet is also being deactivated if either one of the pressure interlocks or the water interlock is being triggered. In a similar manner, we monitor the temperature and humidity in our laboratory via a set point operated Omega CNiTH Dual Temperature and Humidity Sensor unit.[57] An enhanced temperature ($T > 23$ °C) or humidity level (35%) suggests a malfunctioning air conditioning unit. Over hours, limited air cooling can lead to a shut down of air-cooled pumps (magnetically levitated pumps, scroll pumps, and roots pumps) overnight. An increased humidity level can lead to a breakdown of the ceramic insulator of the high voltage feedthrough to the Daly detector (−25 kV). Finally, we incorporated a logic circuit to monitor accidentally released toxic gases such as hydrogen cyanide and carbon monoxide (MDA Scientific; Lifeline II system). Similar to the Liebert 5 kVA UPS system, these monitors switch a relay from its normally open to a closed position. This in turn shuts down the power to the 110 V socket, thus transmitting a page to the person in charge.

IV. SUMMARY

In this article, we presented the design of a modular, versatile interlock system for UHV machines. This system can monitor the pressure (vacuum), the status of the power (power failure, power fluctuations, and scheduled power outages), the operation mode of the pumps (operation versus failure), the flow of cooling, the humidity and temperature levels, as well as the concentration of toxic gases in the laboratory. If any of the set points is triggered, the vacuum machine is protected fully automatically. In addition, the interlock system is interfaced to an automated paging system to transmit a remote message to the person in charge of the laboratory.

ACKNOWLEDGMENTS

This work was supported by the National Science Foundation (CHE-0234461; YG, RIK) and by the US Department of Energy-Basic Energy Sciences (DE-FG02-03ER15411; XG, RIK).

[1] J. P. Toennies, Annu. Rev. Phys. Chem. **55**, 1 (2004).
[2] R. I. Kaiser, Chem. Rev. (Washington, D.C.) **102**, 1309 (2002); A. F. Furlan and G. E. Hall, J. Chem. Phys. **109**, 10390 (1998); A. Furlan, J. Phys. Chem. B **103**, 1550 (1999).
[3] X. Yang and K. Liu, *Modern Trends in Chemical Dynamics* (World Scientific, Singapore, 2003); R. A. Dressler, *Chemical Dynamics in Extreme Environments* (World Scientific, Singapore, 2001).
[4] G. Scoles, *Atomic and Molecular Beam Methods* (Oxford University Press, Oxford, 1988).
[5] A. F. Furlan and G. E. Hall, J. Chem. Phys. **109**, 10390 (1998); A. Furlan, J. Phys. Chem. B **103**, 1550 (1999).
[6] X. Yang and K. Liu, *Modern Trends in Chemical Dynamics* (World Scientific, Singapore, 2003); R. A. Dressler, *Chemical Dynamics in Extreme Environments* (World Scientific, Singapore, 2001); R. I. Kaiser, Chem. Rev. (Washington, D.C.) **102**, 1309 (2002).
[7] K. Liu and A. Wagner, *The Chemical Dynamics and Kinetics of Small Radicals* (World Scientific, Singapore, 1995).
[8] X. Yang and K. Liu, *Modern Trends in Chemical Dynamics* (World Scientific, Singapore, 2003); R. A. Dressler, *Chemical Dynamics in Extreme Environments* (World Scientific, Singapore, 2001).
[9] P. E. Siska, J. Chem. Phys. **59**, 6052 (1973); L. Bewig, U. Buck, S. R. Gandhi, and M. Winter, Rev. Sci. Instrum. **67**, 417 (1996); H. Haberland, U. Buck, and M. Tolle, Rev. Sci. Instrum. **56**, 1712 (1985).
[10] G. Scoles, *Atomic and Molecular Beam Methods* (Oxford University Press, Oxford, 1988).
[11] K. Liu and A. Wagner, *The Chemical Dynamics and Kinetics of Small Radicals* (World Scientific, Singapore, 1995).
[12] P. Casavecchia, N. Balucani, and V. Volpi, Annu. Rev. Phys. Chem. **50**, 347 (1999); P. Casavecchia, Rep. Prog. Phys. **63**, 355 (2000).
[13] Combustion Chemistry: Elementary Reactions to Mascorcopic Processes, Faraday Discussion 119, 2001 (unpublished).
[14] Y. C. Minh and E. F. van Dishoeck, *Astrochemsitry: From Molecular Clouds to Planetary Systems* (International Astronomical Society, San Francisco, 2000).
[15] Y. L. Yung and W. B. DeMore, *Photochemostry of Planetary Atmospheres* (Oxford University Press, Oxford, 1999); M. V. Sykes, *The Future of Solar System Exploration* (International Astronomical Society, San Francisco, 2002).
[16] M. Alagia, N. Balucani, L. Cartechini, and P. Casavecchia, Science **273**, 1519 (1996); D. Skouteris, H. J. Werner, F. J. Aoiz, L. Banares, N. Balucani, and P. Casavecchia, J. Chem. Phys. **114**, 10622 (2001).
[17] B. D. Bean, J. D. Ayers, F. Fernandez-Alonso, and R. N. Zare, J. Chem. Phys. **116**, 6634 (2002).
[18] L. A. Pederson, G. C. Schatz, T. S. Ho, and T. Hollebeek, J. Chem. Phys. **110**, 9091 (1999); N. Balucani, M. Alagia, L. Cartechini, P. Casavecchia, G. G. Volpi, L. A. Pederson, and G. C. Schatz, *ibid.* **105**, 2414 (2001).
[19] M. Alagia, N. Balucani, L. Cartechini, P. Casavecchia, E. H. van Kleef, G. G. Volpi, P. J. Kuntz, and J. J. Sloan, J. Chem. Phys. **108**, 6698 (1998); S. K. Gray, C. Petrongolo, K. Drukker, and G. C. Schatz, Phys. Chem. Chem. Phys. **6**, 1141 (1999).
[20] S. H. Lee and K. Liu, Appl. Phys. B **71**, 627 (2000).
[21] M. Alagia, N. Balucani, P. Casavecchia, D. Stranges, and G. G. Volpi, J. Chem. Phys. **98**, 8341 (1993).
[22] B. R. Strazisar, C. Lin, and H. F. Davis, Science **290**, 5493 (2000).
[23] T. Takayanagi and G. C. Schatz, J. Chem. Phys. **106**, 3227 (1997).
[24] J. M. Bowman and G. C. Schatz, Annu. Rev. Phys. Chem. **46**, 169 (1995).
[25] N. Balucani, P. Casavecchia, F. J. Aoiz, L. Banares, J. F. Castillo, and V. J. Herrero, Mol. Phys. **103**, 1703 (2005); N. Balucani, D. Skouteris, G. Capozza, E. Segoloni, P. Casavecchia, M. H. Alexander, G. Capecchi, and H.-J. Werner, Phys. Chem. Chem. Phys. **6**, 5007 (2004); J. J. Lin, J. Zhou, and K. Liu, Science **300**, 966 (2003); R. T. Skodje, D. Skouteris, D. E. Monolopoulos, S. H. Lee, F. Dong, and K. Liu, Phys. Rev. Lett. **85**, 1206 (2000).
[26] N. Balucani, O. Asvany, Y. T. Lee, R. I. Kaiser, N. Galland, and Y. Hannachi, J. Am. Chem. Soc. **122** 11234 (2000); N. Balucani, O. Asvany, Y. T. Lee, R. I. Kaiser, N. Galland, M. T. Rayez, and Y. Hannachi, J. Comput. Chem. **22**, 1359 (2001).
[27] R. I. Kaiser, Y. T. Lee, and A. G. Suits, J. Chem. Phys. **105**, 8705 (1996); R. I. Kaiser, D. Stranges, H. M. Bevsek, Y. T. Lee, and A. G. Suits, *ibid.* **106**, 4945 (1997); I. Hahndorf, H. Y. Lee, A. M. Mebel, S. H. Lin, Y. T. Lee, and R. I. Kaiser, *ibid.* **113**, 9622 (2000); L. C. L. Huang, H. Y. Lee, A. M. Mebel, S. H. Lin, Y. T. Lee, and R. I. Kaiser, *ibid.* **113**, 9637 (2000); T. N. Lee, H. Y. Lee, A. M. Mebel, and R. I. Kaiser, J. Phys. Chem. A **105**, 1847 (2001); T. L. Nguyen, A. M. Mebel, and R. I. Kaiser, *ibid.* **105**, 3284 (2001); R. I. Kaiser, T. L. Nguyen, T. N. Le, and A. M. Mebel, Astrophys. J., Suppl. **561**, 858 (2001).
[28] R. I. Kaiser, A. M. Mebel, A. H. H. Chang, S. H. Lin, and Y. T. Lee, J. Chem. Phys. **110**, 10330 (1999); N. Balucani, H. Y. Lee, A. Mebel, Y. T. Lee, and R. I. Kaiser, *ibid.* **115**, 5107 (2001).
[29] R. I. Kaiser, Y. T. Lee, and A. G. Suits, J. Chem. Phys. **103**, 10395 (1995); R. I. Kaiser, D. Stranges, Y. T. Lee, and A. G. Suits, *ibid.* **105**, 8721 (1996); R. I. Kaiser, C. Ochsenfeld, M. Head-Gordon, Y. T. Lee, and A. G. Suits, Science **274**, 1508 (1996); J. Chem. Phys. **106**, 1729 (1997); R. I. Kaiser, D. Stranges, Y. T. Lee, and A. G. Suits, Astrophys. J., Suppl. **477**, 982 (1997); C. Ochsenfeld, R. I. Kaiser, A. G. Suits, Y. T. Lee, and M. Head-Gordon, J. Chem. Phys. **106**, 4141 (1997); R. I. Kaiser, C. Ochsenfeld, M. Head-Gordon, and Y. T. Lee, Astrophys. J., Suppl. **510** 784 (1999); R. I. Kaiser, A. M. Mebel, Y. T. Lee, and A. H. H. Chang, J. Chem. Phys. **115**, 5117 (2001).
[30] R. I. Kaiser, I. Hahndorf, L. C. L. Huang, Y. T. Lee, H. F. Bettinger, P. v. R. Schleyer, H. F. Schaefer III, and P. R. Schreiner, J. Chem. Phys. **110**, 6091 (1999); H. F. Bettinger, P. v. R. Schleyer, P. R. Schreiner, H. F. Schaefer III, R. I. Kaiser, and Y. T. Lee, *ibid.* **113**, 4250 (2000); I. Hahndorf, Y. T. Lee, R. I. Kaiser, L. Vereecken, J. Peeters, H. F. Bettinger, P. v. R. Schleyer, and H. F. Schaefer III, *ibid.* **116**, 3248 (2002).
[31] R. I. Kaiser, W. Sun, and A. G. Suits, J. Chem. Phys. **106**, 5288 (1997); R. I. Kaiser, C. Ochsenfeld, M. Head-Gordon, and Y. T. Lee, Science **279**, 1181 (1998); R. I. Kaiser, C. Ochsenfeld, M. Head-Gordon, and Y. T. Lee, J. Chem. Phys. **110**, 2391 (1999); W. D. Geppert, C. Naulin, M. Costes, G. Capozza, L. Cartechini, P. Casavecchia, and G. G. Volpi, *ibid.* **119**, 10607 (2003); D. C. Clary *et al.*, J. Phys. Chem. A **106**, 5541 (2002).
[32] N. Balucani, L. Cartechini, M. Alagia, P. Casavecchia, and G. G. Volpi, J. Phys. Chem. **104**, 5655 (2000).
[33] J. Shu, J. J. Lin, Y. T. Lee, and X. M. Yang, J. Chem. Phys. **115**, 849 (2001); R. L. Gross, X. Liu, and A. G. Suits, Chem. Phys. Lett. **376**, 710 (2003).
[34] R. Z. Hinrichs, P. A. Willis, H. U. Stauffer, J. J. Schroden, and H. F. Davis, J. Chem. Phys. **112**, 4634 (2000); H. U. Stauffer, R. Z. Hinrichs, J. J. Schroden, and H. F. Davis, J. Phys. Chem. **104**, 1107 (2000); R. Z. Hinrichs, J. J. Schroden, and H. F. Davis, *ibid.* **107**, 9284 (2003).
[35] H. U. Stauffer, R. Z. Hinrichs, J. J. Schroden, and H. F. Davis, J. Chem. Phys. **111**, 10758 (1999); J. J. Schroden and H. F. Davis, in *Modern Trends in Chemical Reaction Dynamics, Part 2*, Advanced Series in Physical Chemistry (2004), p. 215; R. Z. Hinrichs, J. J. Schroden, and H. F. Davis, J. Phys. Chem. A **107**, 9284 (2003).
[36] N. Balucani *et al.*, J. Chem. Phys. **111**, 7457 (1999).
[37] L. C. L. Huang, Y. T. Lee, and R. I. Kaiser, J. Chem. Phys. **110**, 7119 (1999); L. C. L. Huang, N. Balucani, Y. T. Lee, R. I. Kaiser, and Y. Osamura, *ibid.* **111**, 2857 (1999); N. Balucani *et al.*, *ibid.* **111**, 7472 (1999); R. I. Kaiser *et al.*, Rev. Sci. Instrum. **70**, 4185 (1999); N. Balucani, O. Asvany, Y. Osamura, L. C. L. Huang, Y. T. Lee, and R. I. Kaiser, Planet. Space Sci. **48**, 447 (2000); N. Balucani, O. Asvany, A. H. H. Chang, S. H. Lin, Y. T. Lee, R. I. Kaiser, and Y. Osamura, J. Chem. Phys. **113**, 8643 (2000); L. C. L. Huang, O. Asvany, A. H. H. Chang, N. Balucani, S. H. Lin, Y. T. Lee, R. I. Kaiser, and Y. Osamura, *ibid.* **113**, 8656 (2000); N. Balucani *et al.*, Astrophys. J., Suppl. **545**, 892 (2000); R. I. Kaiser, Eur. Space Agency [Spec. Publ.] ESA SP **496**, 145 (2001); N. Balucani, R. I. Kaiser, and Y. Osamura, J. Phys. Chem. A **106**, 4301 (2002).
[38] R. I. Kaiser, C. C. Chiong, O. Asvany, Y. T. Lee, F. Stahl, P. v. R. Schleyer, and H. F. Schaefer, J. Chem. Phys. **114**, 3488 (2001); F. Stahl, P. v. R. Schleyer, R. I. Kaiser, Y. T. Lee, and H. F. Schaefer III, *ibid.* **114**, 3476 (2001); R. I. Kaiser, F. Stahl, P. v. R. Schleyer, and H. F. Schaefer, Phys. Chem. Chem. Phys. **13**, 2950 (2002); F. Stahl, P. v. R. Schleyer, H. F. Schaefer, and R. I. Kaiser, Planet. Space Sci. **50**, 685 (2002).

[39] R. I. Kaiser, O. Asvany, Y. T. Lee, H. F. Bettinger, P. v. R. Schleyer, and H. F. Schaefer III, J. Chem. Phys. **112**, 4994 (2000); R. I. Kaiser, O. Asvany, and Y. T. Lee, Planet. Space Sci. **48**, 483 (2000); L. Vereecken, J. Peeters, H. F. Bettinger, P. v. R. Schleyer, H. F. Schaefer III, and R. I. Kaiser, J. Am. Chem. Soc. **124**, 2781 (2002).
[40] X. Liu, J. J. Lin, S. Harich, G. C. Schatz, and X. Yang, Science **289**, 1536 (2000).
[41] M. R. Scholefield, J. H. Choi, S. Goyal, and H. Reisler, Chem. Phys. Lett. **288**, 487 (1998).
[42] X. Yang, J. Lin, Y. T. Lee, D. A. Blank, A. Wodtke, and A. G. Suits, Rev. Sci. Instrum. **68**, 3317 (1997).
[43] P. A. Willis, H. U. Stauffer, R. Z. Hinrichs, and H. F. Davis, Rev. Sci. Instrum. **70**, 2606 (1999).
[44] P. Casavecchia, G. Capozza, E. Segoloni, F. Leonori, N. Balucani, and G. G. Volpi, J. Phys. Chem. A **109**, 3527 (2005); G. Capozza, E. Segoloni, F. Leonori, G. G. Volpi, and P. Casavecchia, J. Chem. Phys. **120**, 4557 (2004).
[45] A. G. Suits and R. E. Continetti, *Imaging in Chemical Dynamics*, ACS Symposium Series (Washington, 2001), Vol. 770.
[46] A. T. J. B. Eppink and D. H. Parker, Rev. Sci. Instrum. **68**, 3477 (1997).
[47] M. Ahmed, D. S. Peterka, and A. G. Suits, Chem. Phys. Lett. **301**, 372 (1999).
[48] M. Ahmed, D. S. Peterka, and A. G. Suits, Phys. Chem. Chem. Phys. **2**, 861 (2000); Chem. Phys. Lett. **317**, 264 (2000).
[49] X. H. Liu, R. L. Gross, and A. G. Suits, J. Chem. Phys. **116**, 5341 (2002); X. H. Liu, R. L. Gross, G. E. Hall, J. T. Muckerman, and A. G. Suits, *ibid.* **117**, 7947 (2002).
[50] A. J. R. Heck and D. W. Chandler, Annu. Rev. Phys. Chem. **46**, 335 (1995); A. Schoffman and D. W. Chandler, Int. Rev. Phys. Chem. **14**, 371 (1995); P. L. Houston, Acc. Chem. Res. **28**, 453 (1995).
[51] L. T. Chu, J. Vac. Sci. Technol. **15**, 201 (1997); N. Kanaya, S. Sakanaka, S. Sato, T. Koide, and S. Saoka, IEEE Trans. Nucl. Sci. **37**, 2 (1990); L. T. Chu, M. T. Leu, and L. F. Keyser, J. Phys. Chem. **97**, 7779 (1993); Y. Satow, K. Ito, and T. Kosuge, Rev. Sci. Instrum. **60**, 1961 (1989); L. H. Dubious, J. Vac. Sci. Technol. A **6**, 162 (1988); S. Xiong, B. Dong, Y. Tan, and Y. Yan, *Proceedings of the International Conference on Accelerator and Large Experimental Physics Control Systems, 1999* (IEEE, New York, 1999), p. 36.
[52] A. Chambers, R. K. Fitch, and B. S. Halliday, *Basic Vacuum Technology* (Institute of Physics, Philadelphia, 1998); J. H. Moore, C. C. Davis, and M. A. Coplan, *Building Scientific Apparatus* (Perseus, Cambridge, 2003); Kent, *Experimental Low Temperature Physics* (MacMillan, London, 1993); W. Pupp and H. K. Hartmann, *Vacuum Technology* (Carl Hanser, Vienna, 1991).
[53] http://www.ascovalves.com
[54] http://www.proteusind.com/Products/flow_switch.html
[55] P. Horowitz and W. Hill, *The Art of Electronics* (Cambridge University Press, Cambridge, 1994).
[56] http://www.liebert. com/dynamic/displayproduct.asp?id=893
[57] www.omega.com/pptst/iTH.html